Global dynamics of models of within-host viral infections including logistic target cell regrowth and innate immune response

Rory Burnham 541554

supervised by James McCaw

May 11, 2018

A thesis submitted to the University of Melbourne School of Mathematics and Statistics in partial fulfilment of the requirements for the degree of Master of Science.

Acknowledgements

Firstly, I would like to thank my supervisor James McCaw. He has provided invaluable guidance throughout my masters. I have always enjoyed our weekly meetings, which worked as a great motivator for me as well as getting me immersed in the world of mathematical biology.

Secondly, I would like to acknowledge Ada Yan for her preliminary work in this area, which has proved invaluable in guiding my thesis. Although I have only met Ada once or twice, I feel as if I know her very well after sifting through much of her unpublished work.

Thirdly, and finally, I would like to thank my family and friends for providing the support I needed throughout this process. I could have not done it without you. Special mention to Phillip Hall for his help in proofreading my thesis.

Contents

1 Abstract

Models of within-host viral infections attempt to quantify the behaviour of a viral infection within a host. These models exhibit different behaviour around fixed points depending on the type of virus that is being modelled. We use this fact as motivation to understand the global stability of particular within-host viral dynamics models. Here, the model of within-host virus dynamics with logistic target cell regrowth is analysed. Dependance on the reproductive ratio, R_0, is established and stable limit cycles are shown to exist for particular parameter domains. The existence of Hopf bifurcations is shown and a bound on the number of bifurcation points established. An innate immunity compartment is then added to the model. Three innate immunity mechanisms are analysed and their qualitative effects on limit cycle solutions demonstrated with the existence of Hopf bifurcations again shown.

2 Introduction

Due to the prevalence of viral infections worldwide and their impact on public health [1, 2], having a sound understanding of their behaviour is vital to treatment and prevention of viral outbreaks. Much of the modelling of viral dynamics has been at the between-host scale, with the SIR model of disease spread now a core concept of mathematical biology and epidemiology [3]. More recently, however, models looking at viral dynamics at the within-host scale have been developed. These models attempt to provide insight into the behaviour of the infection within a host.

Models of within host virus dynamics were first developed in the mid 1990s, such as given in Perelson et al [4]. These models were created specifically to model the viral load in sufferers of HIV [4, 5]. With HIV being a chronic infection, the models were constructed to have solutions which display non-zero viral fixed points. In the 2000s these models were reconstructed and recalibrated to model the viral load curves of other viruses, with particular interest in modellling acute infections such as those displayed by the influenza virus. See [6, 7, 8] for reviews on influenza modelling. From here, modelling of within host viral dynamics has expanded over recent years to include compartments such as immune response as given in[9, 10, 11, 12], and anti-viral drug therapy as given in [13, 5].

The construction of these different models (i.e models of influenza infection versus models of HIV infection) is very similar, yet the behaviour varies significantly between these models. This then begs the question, what is the aspects of there models that dictate such differing outcomes? Furthermore, can this lead to insights about the fundamental differences between acute and endemic viral infections?

Models of influenza infections are finely calibrated to viral load curves taken from clinical trials [14, 9, 10, 11, 12]. In this thesis I will look at some of the basic models of within host virus dynamics [14, 5], cover some of the basic results which have been previously established and from this look to analyse the global dynamics of models of influenza infection.

Firstly, in section 4 I introduce the basic model of within-host viral infections, known as the TIV model, describe how the model is constructed, then show and discuss numerical solutions. In section 5 I outline the mathematical tool kit which will be used throughout this thesis to analyse the TIV model and its adaptations. Section 6 outlines previously described results in the analysis of the TIV model. Subsequently, I will describe conclusions I have reached about the dynamics of adaptations of the TIV

model. Section 7 describes the dynamics of the TIV model with logistic target cell regrowth. Section 8 builds on this analysis by introducing an innate immune response compartment to the model. Section 9 will introduce further models in within-host viral dynamics and, finally, section 10 will discuss the results obtained in this thesis.

3 Biology of viral infections

3.1 Viruses

Viruses are a major issue in global health, with over 50 different viruses known that cause human disease [15]. These diseases can range from the common flu, to endemic infections such as HIV or to deadly acute infections such as Ebola.

Viruses are small parasitic particles (I will refer to these as virions throughout this thesis) which infect host cells [15]. They are made up of chunks of RNA or DNA encased in a protective coating. Viruses differ from other pathogens such as bacteria becuase they are unable to reproduce outside of a host cell [15]. Once a virion has infected a host cell, it is able to reproduce inside that cell, which then expels the newly produced virions back into the system to infect further cells [15]. Different viruses attack different components in the body, with influenza attacking the epithelial (surface) cells of the lungs, HIV attacking CD8+ T cells (a part of a persons immune system) and Hepatitis attacking cells in the liver [15]. Virions are able to invade host cells by having appropriate proteins on the surface of the virus which are able to attach to receptors on the target cells [15].

3.2 Immune response

The immune system plays a large roll in defending a host against infection. The immune system is activated in the presence of antigens (pathogens which induce an immune response). The immune system can be separated into two distinct categories, the innate immune system and the adaptive immune system [15, 16, 17]. The innate immune is the first line of defense against viral (and other) infections. It is innate to most animals [15, 16, 17]. The adaptive immune system produces cells which are specific to a particular virus (or antigen in general) which help clear the virus from the host and protect against future infection [15, 16, 17].

The innate immune system contains three main biological mechanisms, macrophages, interferon and natural killer cells [15, 16, 17]. Macrophages are white blood cells which are able to destroy virions, though macrophages are only able to kill virions outside of a host cell. This makes macrophages less effective than other innate immunity mechanisms, as virions may be held inside infected cells for a period of time before they are released into the system [15]. Interferon works as a warning system to target cells. It binds to the target cell and in the case that the cell is attacked by a virion, the interferon causes the cell and the virion to die, hence suppressing the production of virions and killing infected cells [15]. Interferon can also induce a resistance effect in

target cells, making them less vulnerable to infection by virions [15]. Thirdly, there are natural killer cells, which are produced in the presence of an antigen and kill infected cells [15, 16].

The adaptive immune system contains 2 main mechanisms, antibodies and T cells. Antibodies are produced by blood cells known as B cells. These antibodies contain receptors which are specific to a particular antigen. Antibodies thus have a latent period whilst they "learn" this new receptor [15, 16]. The antibodies are ineffective during this latent period [15, 16]. There are various types of antibodies which work by neutralizing virions and interrupting production in infected cells, as well as marking infected cells for destruction by macrophages[15, 16]. We also have T cells, which are white blood cells produced in the bone marrow and mature in the thymus, thus they also have a latent period in which they are ineffective. They work by "scanning" target cells to determine whether they are infected or not, and killing the ones which are [15, 16].

4 The TIV Model

In models of within-host virus dynamics, we wish to understand the behaviour of the 3 basic components of a viral infection [14, 6, 18, 5]. We have T, the number of healthy cells which are susceptible to infection (known as target cells), I, the number of cells which have been infected, and V, the number of virion particles which are produced by infected cells and infect target cells [14].
Initially we will have some injection of virions into a virus-free system. Target cells become infected when they come into contact with virions. When this occurs, a cell transitions from the T state to the I state. Once a cell is infected it is now capable of producing further virions. We assume that infected cells produce virions at some constant rate, and infected cells and virions decay at their own respective rates [14]. For the moment we will not introduce decay of target cells, this will be discussed in section 6. These state transitions are summarised by the equations given below in 4.1 [19].

$$\mathrm{T} + \mathrm{V} \xrightarrow{\beta} \mathrm{I} \tag{4.1a}$$

$$\mathrm{I} \xrightarrow{\mathrm{p}} \mathrm{I} + \mathrm{V} \tag{4.1b}$$

$$\mathrm{I} \xrightarrow{\delta_\mathrm{I}} \varnothing \tag{4.1c}$$

$$\mathrm{V} \xrightarrow{\mathrm{c}} \varnothing\,. \tag{4.1d}$$

Here, $\varnothing$ is the empty set. Virions and cells transitioning to the empty set represents the decay (death) of cells.
Now, we assume that the interaction of virions and target cells obeys a concept known as the law of mass action [8], which states that the number of interactions between target cells and virions will be proportional to the product of the population of the two reactants. From these simplifications of the biology we can now construct a set of ordinary differential equations known as the TIV model,

$$\frac{dT}{dt} = -\beta TV, \tag{4.2a}$$

$$\frac{dI}{dt} = \beta TV - \delta_I I, \tag{4.2b}$$

$$\frac{dV}{dt} = pI - cV. \tag{4.2c}$$

β is our infectivity parameter, given in units $M^{-1}t^{-1}$. M is dependant on what the the model is calibrated to, usually being some measure of virion population or concentration. β gives the number of target cells which are infected by a single virion per

unit time. δ_I and c, given in units t^{-1}, are the death rates of infected cells and virions respectively, and p, given in units t^{-1}, is the rate of production of virions by infected cells.

Due to the non-linearity of this system, as of yet there is no analytic solution to equation 4.2. Because of this we will proceed to analyse this and the following models numerically. This is done in MATLAB R2017a using the ode15s differential equation solver.

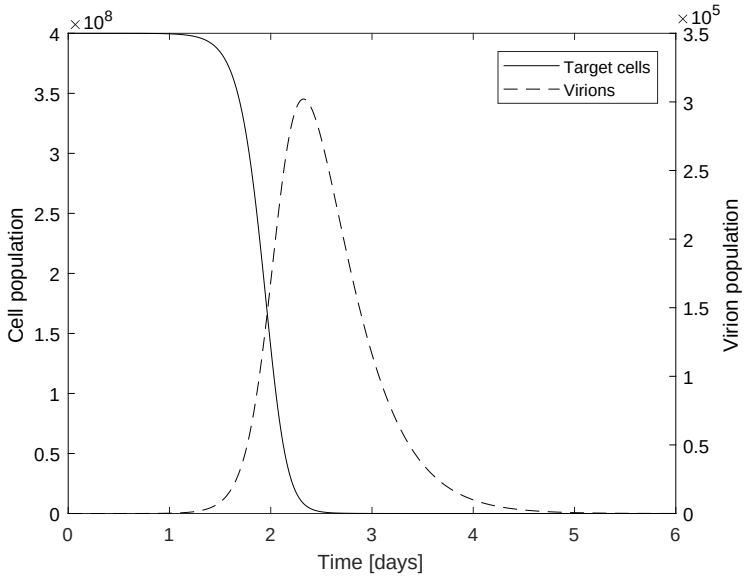

Figure 4.1: Simulation of the TIV model using parameter values given in table 4.1.

T_0	V_0	β	δ_I	p	c
4e8	3.5e-1	3.4e-5	3.4	7.9e-3	3

Table 4.1: Baseline parameter values for the TIV model given in [14].

Running a simulation using the base parameter values given in table 4.1 gives us the result show in figure 4.1. The system is stimulated by a small number of virions initially to create an infection, at which point target cells become infected quite rapidly and hence production of virions is stimulated. The system then reaches a critical point, represented by the peak of the viral curve, where there is no longer a sufficient number of target cells to maintain virion growth. These dynamics are controlled by a value, R_0, which will be described in section 6. This is known as a target cell limited model, as there is only a finite pool of target cells to feed the infection.

To increase the clarity of figure 4.1, the curve of infected cells has been omitted. This curve follows a similar path to that of the virions, with the peak of infected cells happening slightly earlier than that of virions. Throughout the remainder of this thesis I will be focusing on the dynamics of the virions and the target cells, as their behaviour is largely indicative of the dynamics of an infection.

5 Mathematical preliminaries

A dynamical system is a system which evolves in time. Here we will be focusing on deterministic systems. In deterministic systems, the future state of the system is completely dictated by the current state.
In this paper we will be considering models which are governed by a set of ordinary differential equations which take the form

$$\frac{d\mathbf{x}}{dt} = \mathbf{f}(\mathbf{x}), \tag{5.1}$$

where $\mathbf{x} = \begin{bmatrix} x_1 \\ x_2 \\ \vdots \\ x_n \end{bmatrix}$ and $\mathbf{f}(\mathbf{x}) = \begin{bmatrix} f_1(x_1, x_2, \ldots, x_n) \\ f_2(x_1, x_2, \ldots, x_n) \\ \vdots \\ f_n(x_1, x_2, \ldots, x_n) \end{bmatrix}$.
Generally, the vector of functions, $\mathbf{f}(\mathbf{x})$, contains non-linear terms making it difficult to construct an analytic solution to the equations. This means in order to to gain insight into the behaviour of the models we analyse the long term asymptotic behaviour.

5.1 Linear Stability Analysis

The following derivation is motivated by explanations given in [20, 21, 22].

Fixed points are defined as points in the system, $\bar{\mathbf{x}}$, which satisfy

$$\frac{d\bar{\mathbf{x}}}{dt} = \mathbf{f}(\bar{\mathbf{x}}) = 0. \tag{5.2}$$

In other words, these are points at which the system remains (with the time derivative being 0). Our goal here is to determine how the system will evolve if slightly perturbed from these fixed points.

Let $\mathbf{x} = \bar{\mathbf{x}} + \delta\mathbf{x}$ where $\delta\mathbf{x} = \begin{bmatrix} \delta x_1 \\ \delta x_2 \\ \vdots \\ \delta x_n \end{bmatrix}$ is some perturbation away from the fixed point.

We now substitute this into 5.1, yielding

$$\frac{d(\bar{\mathbf{x}} + \delta\mathbf{x})}{dt} = \mathbf{f}(\bar{\mathbf{x}} + \delta\mathbf{x})$$
$$\Rightarrow \frac{d\bar{\mathbf{x}}}{dt} + \frac{d(\delta\mathbf{x})}{dt} = \mathbf{f}(\bar{\mathbf{x}} + \delta\mathbf{x})$$

Doing a Taylor expansion on $\mathbf{f}(\bar{\mathbf{x}} + \delta\mathbf{x})$ around the point $\bar{\mathbf{x}} + \delta\mathbf{x} = \bar{\mathbf{x}}$ gives

$$\frac{d\bar{\mathbf{x}}}{dt} + \frac{d(\delta\mathbf{x})}{dt} = \mathbf{f}(\bar{\mathbf{x}}) + \nabla\mathbf{f}(\mathbf{x})|_{\mathbf{x}=\bar{\mathbf{x}}}\delta\mathbf{x} + O((\delta\mathbf{x})^2). \tag{5.3}$$

From equation 5.2, we know $\mathbf{f}(\bar{\mathbf{x}})$ and $d\bar{\mathbf{x}}/dt$ vanish. We also now assume that $\delta x_i \ll 1,\ i = 1 \dots n$, and so can discard $O((\delta\mathbf{x})^2)$ terms (here $(\delta\mathbf{x})^2$ is a vector where each element is squared). This leaves us with a differential equation in terms of our perturbation

$$\frac{d(\delta\mathbf{x})}{dt} = J(\bar{\mathbf{x}})\delta\mathbf{x}, \tag{5.4}$$

where

$$J(\mathbf{x})_{ij} = \nabla\mathbf{f}(\mathbf{x})_{ij} = \frac{\partial f_i(\mathbf{x})}{\partial x_j},\ i, j = 1 \dots n$$

is the matrix of partial derivatives, known as the Jacobian of the system.
Equation 5.4 is just a system of linear, first order ODEs. This has the general solution

$$\delta\mathbf{x} = \sum_{i=1}^{n} a_i \mathbf{v}_i \exp(\lambda_i t) \tag{5.5}$$

where $\mathbf{v}_i$ and λ_i are the eigenvectors and eigenvalues of the Jacobian, respectively, and a_i is determined by initial conditions.

From the solution to our perturbation ODE, equation 5.5, it is obvious that if we wish this perturbation to decrease with time we require all eigenvalues of $J(\bar{\mathbf{x}})$ to have negative real parts, i.e. $\mathrm{Re}(\lambda_i) < 0\ \forall\ i = 1 \dots n$. This is known as a stable fixed point as the system will tend towards this point as time increases. Conversely, if there exists an eigenvalue λ_i such that $\mathrm{Re}(\lambda_i) > 0$ then the perturbation will increase with time. These are known as unstable fixed points as the system will tend away from these points as time increases.

5.2 Bifurcations

Analysing the stability of the fixed points provides insight into the system's long term behaviour. Our next question is how does this asymptotic behaviour change when we vary the parameters of the system?

A bifurcation point in a dynamical system is a point in which the qualitative nature of the fixed points changes dependant on the parameters of the system. Following are some examples of different bifurcations relevant to within host viral dynamics, specifically the TIV model, and the mathematical contexts in which they occur. See Strogatz [20] and Edelstein-Keshet [21] for further discussion of the following types of bifurcations, and explanations of other bifurcations which can occur in dynamical systems.

5.2.1 Transcritical bifurcation

Let us consider the basic logistic growth equation

$$\frac{dx}{dt} = rx - x^2.$$

We are interested in how the fixed points of the system above are affected by the value of the growth parameter r. We have two fixed points, $\bar{x} = 0$ and $\bar{x} = r$.

Since this is a simple 1D system, the Jabobian is simply given by the scalar $J(x) = r - 2x$. Hence $J(0) = r$ and $J(r) = -r$. For $r < 0$ we have $J(0) < 0$ and $J(r) > 0$. Conversely, for $r > 0$, $J(0) > 0$ and $J(r) < 0$.
We can see that at the point $r = 0$, we have an exchange of stability between the 2 fixed points. This is known as a transcritical bifurcation. These results are summarised in figure 5.1.

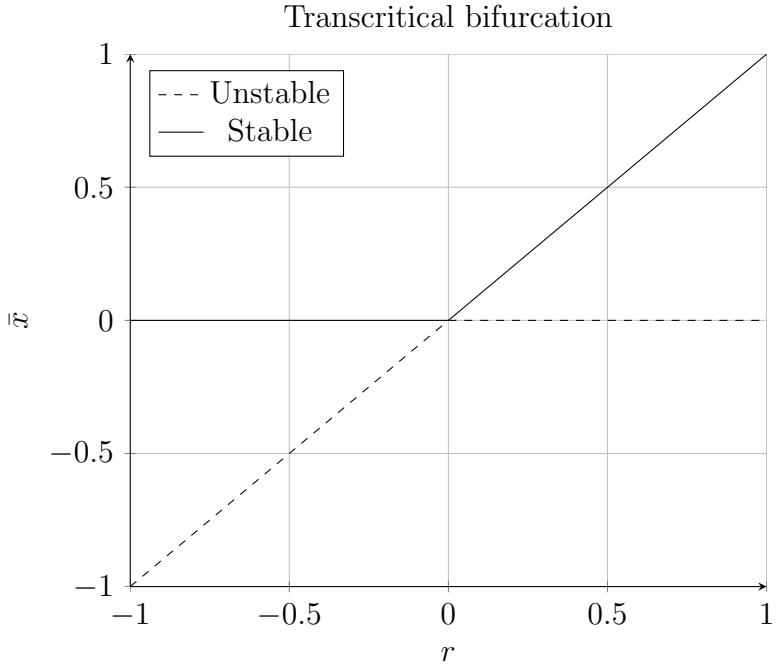

Figure 5.1

At the point $r = 0$ we have an exchange of stability between $\bar{x} = 0$ and $\bar{x} = r$, with the former becoming unstable and vice versa. More generally, for systems of arbitrary dimensions, a transcritical bifurcation will occur when two fixed points, one stable and one unstable, intersect, and there is an exchange of stability. For the previously stable fixed point, one of the eigenvalues will have its real part transition from negative to positive. For the previously unstable fixed point, there will be one eigenvalue in which the real part passes from positive to negative, and we must have that all the other eigenvalues have real parts less than zero.

5.2.2 Hopf bifurcation

Firstly, we need to define the concept of a limit cycle.

Consider some $2D$ system,

$$\frac{dx}{dt} = f(x, y), \tag{5.6a}$$

$$\frac{dy}{dt} = g(x, y). \tag{5.6b}$$

A limit cycle is a solution which spirals towards a closed trajectory in the x, y plane around a fixed point $(\bar{x}, \bar{y})$. If we plot the solution to equations 5.6 and see the solution

spiral towards a closed trajectory as time progresses, this is known as a stable limit cycle. If, on the other hand, the solution spirals away from a closed trajectory around a fixed point, this is known as an unstable limit cycle. Another way to think about an unstable limit cycle is if we run time backwards it will spiral towards a closed trajectory.

The next question is in what contexts do these limit cycle solutions arise? This brings us to the concept of a Hopf bifurcation. In the system given by equation 5.6, for us to have a stable fixed point we require $\mathrm{Re}(\lambda) < 0$ for all eigenvalues of the system evaluated at the fixed point. In the $2D$ case we can either have two real eigenvalues, or we can have complex conjugate eigenvalues. For complex conjugate eigenvalues, the system will have damped oscillations towards the fixed point $(\bar{x}, \bar{y})$. Suppose the value of these eigenvalues is dependant on some parameter α. Our eigenvalues can be written $\lambda_{\pm} = a(\alpha) \pm ib(\alpha)$. Let $\bar{\alpha}$ be a point such that $a(\bar{\alpha}) = 0$. For $\alpha < \bar{\alpha}$, $a(\alpha) < 0$ and we have damped oscillations towards the fixed point. At $\alpha = \bar{\alpha}$, the eigenvalues have lost stability and limit cycle solutions emerge, oscillating around the fixed point $(\bar{x}, \bar{y})$. This is known as a supercritical Hopf bifurcation. Supercritical Hopf bifurcations can also occur when the parameter is decreased and stable limit cycles occur around an unstable fixed point for $\alpha < \bar{\alpha}$. A subcritical Hopf bifurcation is when we start with an unstable fixed point $(\bar{x}, \bar{y})$. As α is increased and passes through the bifurcation point $\alpha = \bar{\alpha}$, the fixed point gains stability an unstable limit cycles emerges around this point. As with supercritical bifurcations, this can also occur as the parameter is decreased.

We can extend this concept to systems of arbitrary dimension. Assume we have some stable fixed point. If the Jacobian evaluated at the fixed point has a pair of complex conjugate eigenvalues dependant on some parameter, as these eigenvalues cross the imaginary axis in the complex plane, a Hopf bifurcation occurs.

Both Hopf and transcritical bifurcations involve an eigenvalue having a real part pass through zero. The distinction is that transcritical bifurcations involve an exchange of stability between two distinct fixed points which both have eigenvalues that pass through zero. In the case of a Hopf bifurcation, we are still looking at the same fixed point, but it has lost stability via complex conjugate eigenvalues passing through zero and stable limit cycles emerging or disappearing around the same fixed point.

5.3 Routh-Hurwitz stability criterion

In the study of dynamical systems, we are often analysing characteristic equations of Jacobians to determine the stability of a fixed point of a system of ordinary differential equations. It is often difficult to infer information about the stability of the fixed point

as analytic solutions get very complex as the degree of the polynomial increases (and the degree of the system).

The Routh-Hurwitz stability criterion give us a series of inequalities which allow us to infer information about the value of the roots of these polynomials without explicit calculation. This definition is motivated by explanations of the Routh-Hurwitz criterion in Edelstein-Keshset [21] and Murray [22].

In general, for an n dimensional system, we will get a characteristic equation of the Jacobian in the form

$$C_n(\lambda) = \lambda^n + a_1\lambda^{n-1} + \cdots + a_{n-1}\lambda + a_n \tag{5.7}$$

where $a_1, \ldots, a_n$ are real valued functions of the parameters of the system. For stability of the system we require $\mathrm{Re}(\lambda) < 0$ for all solutions of $C(\lambda) = 0$.

We now define the Hurwitz matrix of a polynomial. The Hurwitz matrix of equation 5.7 is given by

$$H_n = \begin{Bmatrix} a_1 & a_3 & a_5 & \ldots & \ldots & \ldots & 0 & 0 & 0 \\ 1 & a_2 & a_4 & & & & \vdots & \vdots & \vdots \\ 0 & a_1 & a_3 & & & & \vdots & \vdots & \vdots \\ \vdots & 1 & a_2 & \ddots & & & 0 & \vdots & \vdots \\ \vdots & 0 & a_1 & & \ddots & & a_n & \vdots & \vdots \\ \vdots & \vdots & 1 & & & \ddots & a_{n-1} & 0 & \vdots \\ \vdots & \vdots & 0 & & & & a_{n-2} & a_n & \vdots \\ \vdots & \vdots & \vdots & & & & a_{n-3} & a_{n-1} & 0 \\ 0 & 0 & 0 & \ldots & \ldots & \ldots & a_{n-4} & a_{n-2} & a_n \end{Bmatrix}. \tag{5.8}$$

For the roots of equation 5.7 to all have real parts less than zero, we require

$$a_n > 0 \text{ and } |H_k| > 0,\ k = 1 \ldots n-1 \tag{5.9}$$

where H_k is a k by k matrix formed using the coefficients of equation 5.7. As an example, for the equation $\lambda^4 + a_1\lambda^3 + a_2\lambda^2 + a_3\lambda + a_4 = 0$ to have all roots with negative real parts we need

$$\begin{vmatrix} a_1 & a_3 & 0 \\ 1 & a_2 & a_4 \\ 0 & a_1 & a_3 \end{vmatrix} > 0, \ \begin{vmatrix} a_1 & a_3 \\ 1 & a_2 \end{vmatrix} > 0, \ a_1 > 0, \ a_4 > 0.$$

6 Global dynamics of the TIV model

We wish to use the tools outlined in the previous section to analyse the fixed points and stability of the TIV model and hopefully gain insight into its global dynamics. This section contains previously realised results as seen in [14, 5] and summarised in the review papers [6, 18].

6.1 The reproductive ratio R_0

Now let us consider the fixed points of equations 4.2. Setting the differential equations to zero gives us $\bar{I} = \bar{V} = 0$ in all cases. Hence, the system will always tend towards a virus free fixed point. From this we ask the question-given an initial injection of virions into the system, V_0, in what conditions will the number of virions grow to form an infection, and in what conditions will the virions die off before an infection can occur. For an infection to occur, we require that each initial virion result in the creation of more than one virion in its lifetime. This number is known as the reproductive ratio, R_0 (this ratio is analogous to the reproductive ratio in epidemiology [3]).

R_0 can be heuristically derived by consideration of the parameters and some dimensional analysis [14, 6, 8, 5]. Each virion infects βT target cells per unit time, and each infected cell creates p virions per unit time. Now, we consider that virions and infected cells have expected lifespans of $1/c$ and $1/\delta_I$ respectively. Finally, we are interested in what this value is at the time of infection, so we take $T = T_0$ and obtain

$$R_0 = \frac{p\beta T_0}{c\delta_I}.$$

For a more rigorous derivation or R_0, we will proceed by performing a linear stability analysis (as defined in section 5). Consider the fixed points of equation 4.2. As mentioned above we have $\bar{V} = \bar{I} = 0$. Our value for $\bar{T}$ depends on how many target cells have been infected before the population of virions dies off, so, instead of having a single fixed point, we have a line of fixed points, $\bar{T} \in [0, T_0]$, which is dependent on the parameters of the system. To overcome this, let us linearise the system around the point $T = T_0$ and consider under what conditions I and V go to zero. The system reduces to

$$\frac{dI}{dt} = \beta T_0 V - \delta_I I, \tag{6.1a}$$

$$\frac{dV}{dt} = pI - cV. \tag{6.1b}$$

This gives us the following Jacobian,

$$J = \begin{bmatrix} -\delta_I & \beta T_0 \\ p & -c \end{bmatrix}. \tag{6.2}$$

The characteristic equation of J is given by

$$C(\lambda) = \lambda^2 + (\delta_I + c)\lambda + c\delta_I - p\beta T_0. \tag{6.3}$$

Setting $C(\lambda) = 0$ and solving gives us the eigenvalues of the Jacobian evaluated at $\bar{V} = \bar{I} = 0$.

$$\lambda_1 = \frac{1}{2}\left(-c - \delta_I - \sqrt{4p\beta T_0 + c^2 - 2c\delta_I + \delta_I^2}\right), \tag{6.4a}$$

$$\lambda_2 = \frac{1}{2}\left(-c - \delta_I + \sqrt{4p\beta T_0 + c^2 - 2c\delta_I + \delta_I^2}\right). \tag{6.4b}$$

For stability we require $\lambda_1 < 0$ and $\lambda_2 < 0$. This can only occur when

$$\begin{aligned} & c + \delta_I > \sqrt{4p\beta T_0 + (c - \delta_I)^2} \\ \Rightarrow\ & c^2 + 2c\delta_I + \delta_I^2 > 4p\beta T_0 + c^2 - 2c\delta_I + \delta_I^2 \\ \Rightarrow\ & c\delta_I > p\beta T_0 \\ \Rightarrow\ & \frac{p\beta T_0}{c\delta_I} < 1 \end{aligned}$$

and we have again arrived at our the same R_0 value.

If $R_0 < 1$, then each virion does not result in the creation of more than 1 further virion, meaning $dV/dt < 0$ and hence the virions die out. On the contrary, if $R_0 > 1$, then at the time of infection we have $dV/dt > 0$, the number of virions grow meaning an infection is sustained.

R_0 can be generalised to be a constantly evolving ratio by replacing T_0 by the value of $T(t)$. We can see in figure 4.1 that the virion population reaches a maximum then dies off. It is at this point that $R_0(t) = 1$, after which $R_0(t) < 1$.

6.2 Constant target cell regrowth

In this section I will be discussing and reproducing results arrived at in [5].

The TIV model presented in section 4 can produce an accurate viral load curve for a short term influenza infection, but has very rudimentary dynamical properties and could not be used to model a longer term/endemic infection. To do this we need to introduce target cell turnover so there is a constant supply of cells to feed the infection.

To do this, let us introduce a growth term (σ) and a death term ($\delta_T T$) to the differential equation for T in equation 4.2. σ is the constant growth rate of target cells produced by the body, given in units Mt^{-1}, and δ_T is the death rate of target cells, given in units t^{-1}. The new model is

$$\frac{dT}{dt} = \sigma - \beta TV - \delta_T T \tag{6.5a}$$
$$\frac{dI}{dt} = \beta TV - \delta_I I \tag{6.5b}$$
$$\frac{dV}{dt} = pI - cV. \tag{6.5c}$$

This model is presented in [5], with the baseline parameter values given in table 6.1.

T_0	V_0	σ	β	δ_I	δ_T	p	c
1e6	10	1e5	2e-7	0.5	0.1	100	5

Table 6.1: Baseline parameter values for TIV model with constant target cell regrowth.

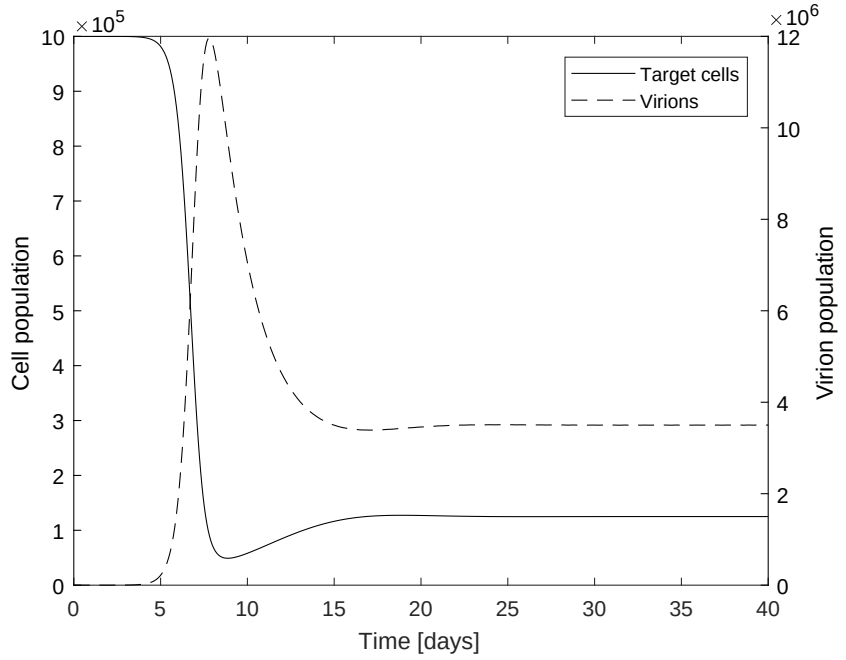

Figure 6.1

As in figure 4.1 we see rapid growth in virions until a peak value is reached, at which point there is insufficient target cells to maintain virion population growth. However, due to the constant growth of target cells, the death of virions stabilises and the curve tends towards a non-zero virus fixed point.

6.2.1 Stability analysis

Now, as before in the basic TIV model, whether an infection is sustained or not is governed by R_0. For the TIV model with constant target cell regrowth, in a virus free state ($V = I = 0$), we have

$$\frac{dT}{dt} = \sigma - \delta_T T \tag{6.6}$$

which has the solution

$$T = \frac{\sigma}{\delta_T}. \tag{6.7}$$

Thus our R_0 is the same as before, but now we set $T_0 = \sigma/\delta_T$, giving us

$$R_0 = \frac{p\beta\sigma}{c\delta_I\delta_T}. \tag{6.8}$$

Once again we can more rigorously derive this R_0 dependence. By inspection it is easily

verifiable that one fixed point of 6.5 is given by $(\bar{T}, \bar{I}, \bar{V}) = (\sigma/\delta_T, 0, 0)$. We can also derive a non-zero virus fixed point. If we set all the equations defined in 6.5 to be zero we obtain

$$\sigma - \beta T\bar{V} - \delta_T\bar{T} = 0, \tag{6.9a}$$
$$\beta\bar{T}\bar{V} - \delta_I\bar{I} = 0, \tag{6.9b}$$
$$p\bar{I} - c\bar{V} = 0. \tag{6.9c}$$

Equation 6.9c gives us $\bar{V} = p\bar{I}/c$. Substituting this into equation 6.9b gives $\bar{T} = c\delta_I/\beta p$. Now, again substituting into equation 6.9a gives $\bar{I} = (\sigma\beta p - \delta_I\delta_T c)/\beta p\delta_I$. Hence the non-zero virus fixed point is given by

$$(\bar{T}, \bar{I}, \bar{V}) = \left(\frac{c\delta_I}{\beta p}, \frac{\sigma\beta p - \delta_I\delta_T c}{\beta p\delta_I}, \frac{\sigma\beta p - \delta_I\delta_T c}{\beta\delta_I c}\right). \tag{6.10}$$

Note that for this fixed point to be a physically relevant solution, we require $\sigma\beta p - \delta_I\delta_T c > 0$ (another indicator of R_0 dependence).

The Jacobian of equation 6.5 is given by

$$J = \begin{bmatrix} -\beta V - \delta_T & 0 & -\beta T \\ \beta V & -\delta_I & \beta T \\ 0 & p & -c \end{bmatrix}, \tag{6.11}$$

which has a characteristic equation given by

$$C(\lambda) = \lambda^3 + a_1\lambda^2 + a_2\lambda + a_3 \tag{6.12}$$

where

$$a_1 = \beta V + c + \delta_I + \delta_T, \tag{6.13a}$$
$$a_2 = \delta_I\delta_T + c\delta_T + c\delta_I + \beta\delta_I V + c\beta V - p\beta T, \tag{6.13b}$$
$$a_3 = c\delta_I\delta_T + c\beta\delta_I V - p\beta\delta_T T. \tag{6.13c}$$

Substituting in $(T, I, V) = (\sigma/\delta_T, 0, 0)$ gives

$$a_1 = c + \delta_I + \delta_T, \tag{6.14a}$$
$$a_2 = \delta_I\delta_T + c\delta_T + c\delta_I - p\beta\sigma/\delta_T, \tag{6.14b}$$
$$a_3 = c\delta_I\delta_T - p\beta\sigma. \tag{6.14c}$$

For fixed point stability ($Re(\lambda) < 0$ for all eigenvalues of J evaluated at $(T, I, V) = (\sigma/\delta_T, 0, 0)$), by the Routh-Hurwitz stability criterion (defined by equation 5.9) we require

$$a_1 > 0,\ a_3 > 0 \text{ and } a_1 a_2 - a_3 > 0.$$

Since all the parameters are positive, real numbers, it is obvious that $a_1 > 0$. Looking at the third criterion, we get

$$\begin{aligned} a_1 a_2 &= 3c\delta_I\delta_T + c^2\delta_I + c^2\delta_T + c\delta_I^2 + \delta_I^2\delta_T + c\delta_T^2 + \delta_I\delta_T^2 - (c + \delta_I + \delta_T)p\beta\sigma/\delta_T \\ &= 2c\delta_I\delta_T + c^2\delta_I + c^2\delta_T + c\delta_I^2 + \delta_I^2\delta_T + c\delta_T^2 + \delta_I\delta_T^2 - (c + \delta_I)p\beta\sigma/\delta_T + a_3 \\ \Rightarrow a_1 a_2 - a_3 &= 2c\delta_I\delta_T + c^2\delta_I + c^2\delta_T + c\delta_I^2 + \delta_I^2\delta_T + c\delta_T^2 + \delta_I\delta_T^2 - (c + \delta_I)p\beta\sigma/\delta_T. \end{aligned}$$

We need to show

$$2c\delta_I\delta_T + c^2\delta_I + c^2\delta_T + c\delta_I^2 + \delta_I^2\delta_T + c\delta_T^2 + \delta_I\delta_T^2 - (c + \delta_I)p\beta\sigma/\delta_T > 0.$$

Pulling out a factor of $1/\delta_T$ we obtain

$$\begin{aligned} a_1 a_2 - a_3 =& \frac{1}{\delta_T}\left(2c\delta_I + c^2\delta_I\delta_T + c^2\delta_T^2 + c\delta_I^2\delta_T + \delta_I^2\delta_T^2 + c\delta_T^3 + \delta_I\delta_T^3 - (c + \delta_I)p\beta\sigma\right) \\ =& \frac{1}{\delta_T}(2c\delta_I + c^2\delta_T^2 + \delta_I^2\delta_T^2 + c\delta_T^3 + \delta_I\delta_T^3 + (c + \delta_I)(c\delta_I\delta_T - p\beta\sigma)) \\ =& \frac{1}{\delta_T}(2c\delta_I + c^2\delta_T^2 + \delta_I^2\delta_T^2 + c\delta_T^3 + \delta_I\delta_T^3 + (c + \delta_I)a_3). \end{aligned}$$

Hence, all 3 criteria will be satisfied if $a_3 > 0$. Rearranging, we arrive again at our previously derived ratio for R_0,

$$R_0 = \frac{p\beta\sigma}{c\delta_I\delta_T} < 1.$$

As R_0 passes through 1 from below, we will get a change in at least 1 of the eigenvalues, with the value changing from $Re(\lambda) < 0$ to $Re(\lambda) > 0$. This is a Transcritical bifurcation, with an exchange of stability between the zero-virus and endemic virus fixed points.

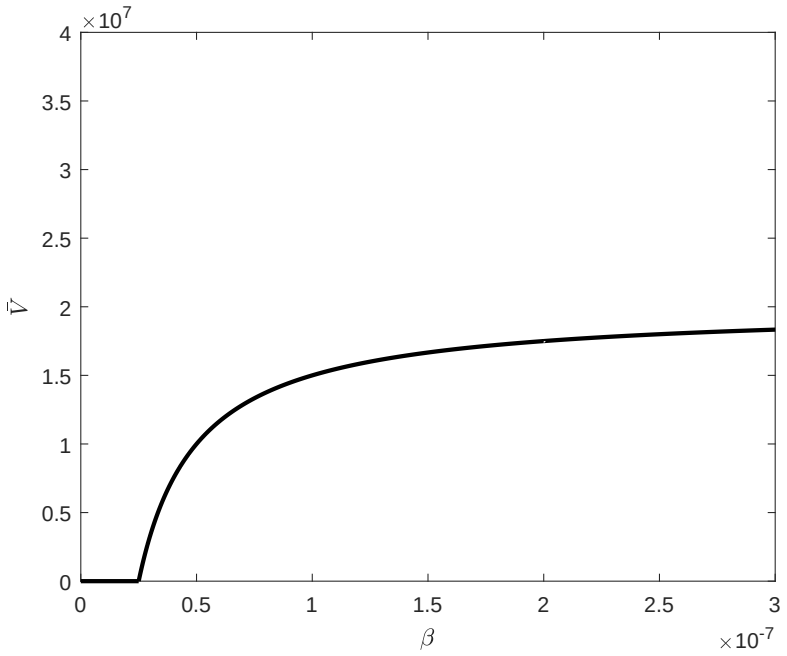

Figure 6.2: Here we isolate the parameter β which is varied whilst all other parameters remain fixed. We can see the point at which the transcritical bifurcation occurs and there is an exchange of stability between the zero virus and non-zero virus fixed points. This occurs at $\beta = 2.5\text{e-}8$ which corresponds to $R_0 = 1$.

How do we interpret this biologically? We can split the parameters into 2 categories, those in the numerator of R_0 and those in the denominator. The infectivity of the virus, β, the budding rate of infected cells, p, and the target cell regrowth rate, σ, are all directly proportional to R_0. As they increase, leaving the other parameters fixed, they will cause the system to undergo a transcritical bifurcation, meaning the zero virus fixed point becomes unstable and a non-zero viral fixed point gains stability.
Conversely, if we look at the decay rates of target cells, infected cells and virions, δ_T, δ_I and c, respectively, we notice they are all inversely proportional to R_0, meaning as they increase, and pass through the $R_0 = 1$ threshold, they will cause the non-zero viral fixed point to become unstable and the zero viral fixed point to gain stability. So, to clear the virus we either want to increase c, δ_I or δ_T, or decrease β, p or σ.

7 Logistic target cell regrowth

Results obtained in this section were motivated by unpublished work undertaken by Ada Yan in her PhD work at the University of Melbourne.

As shown in section 6, in order to induce a non-zero virus fixed point in the TIV model we need to introduce turnover of target cells. Constant target cell regrowth is appropriate for modelling a virus such as HIV as the system very quickly reaches non-zero virus fixed point, as one would expect to see in a HIV infection [4, 5]. This, however, is not appropriate for modelling acute viral infections such as influenza, in which the host is infected for a short period of time before the virus dies out. In order to model influenza with a target cell regrowth term, we introduce logistic target cell regrowth to the TIV model. Models given in [11, 9, 10] use logistic regrowth of target cells to model acute influenza infections. In this section I will present my results about the global dynamics of the TIV model with logistic target cell regrowth.

Our differential equation for T including logistic regrowth is

$$\frac{dT}{dt} = \sigma T\left(1 - \frac{T+I}{T_0}\right) - \beta TV \tag{7.1}$$

The logistic regrowth works by limiting the growth of target cells close to some carrying capacity, in this case T_0 (the number of target cells in the system in a virus free state). The cells regrow at a rate proportional to T (this rate is governed by the parameter σ, given in units t^{-1}), but cell growth is then limited by how close the cell count is to the carrying capacity. We include infected cells, I, in this count as an infected cell will take up the same amount of space as a healthy cell.
The updated model is now given by

$$\frac{dT}{dt} = \sigma T\left(1 - \frac{T+I}{T_0}\right) - \beta TV \tag{7.2a}$$

$$\frac{dI}{dt} = \beta TV - \delta_I I \tag{7.2b}$$

$$\frac{dV}{dt} = pI - cV. \tag{7.2c}$$

This is a simplification of the model given in [10]. Note that we have omitted the decay of target cells term $\delta_T T$. Due to the nature of logistic growth, target cells can never exceed the carrying capacity T_0. This term was required in the case of constant target cell regrowth, however, as we would have had unbounded growth of target cells otherwise.

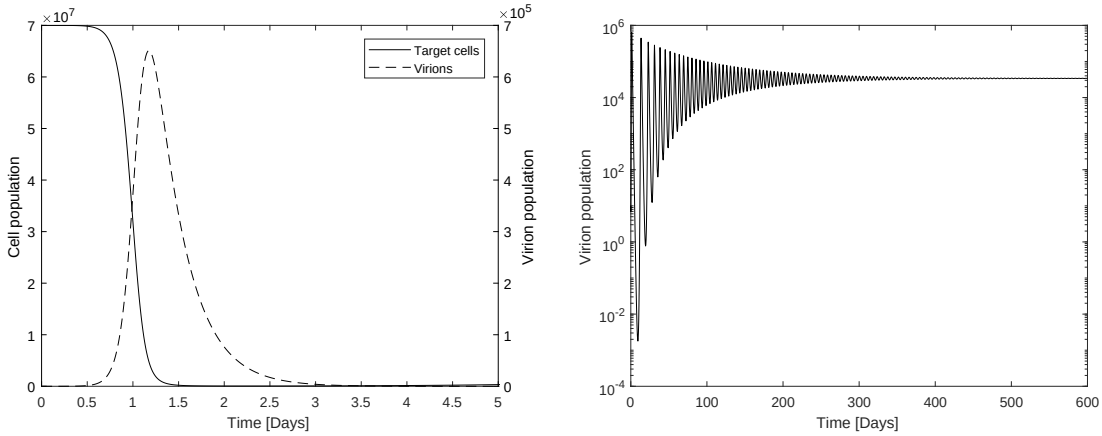

(a) (b)

Figure 7.1

T_0	V_0	σ	β	δ_I	p	c
7e7	10	0.8	2e-5	3	0.35	20

Table 7.1: Parameter values taken from [10]

Figure 7.1a shows the initial transient for the TIV model with logistic target cell regrowth. Note its similarity with the curves shown in figure 4.1. Figure 7.1b shows the convergence to a stable fixed point via damped oscillations over a period of 600 days.

Initially, $(T + I)/T_0 \approx 1$. As target cells transform into infected cells, this ratio will stay roughly the same value. It is only when infected cells start dying in larger numbers (I gets large) that this ratio will start decreasing, at which point production of target cells will be stimulated again. This is evidenced by the trough in between peaks in viral load as shown in figure 7.1b. This trough is what allows acute infections like influenza to be modelled by the TIV model with logistic target cell regrowth.

7.1 Initial transient and trough depth

As there is a deep trough after the initial transient as seen in figure 7.1, it is an appropriate system for modelling acute infections such as influenza. At these small values stochastic effects would dominate and extinction is likely [10], meaning the infection dies out before a fixed point can be reached.

If we compare the initial transient in figure 7.1a with the curve in the case that $\sigma = 0$, we see that they are essentially the same.

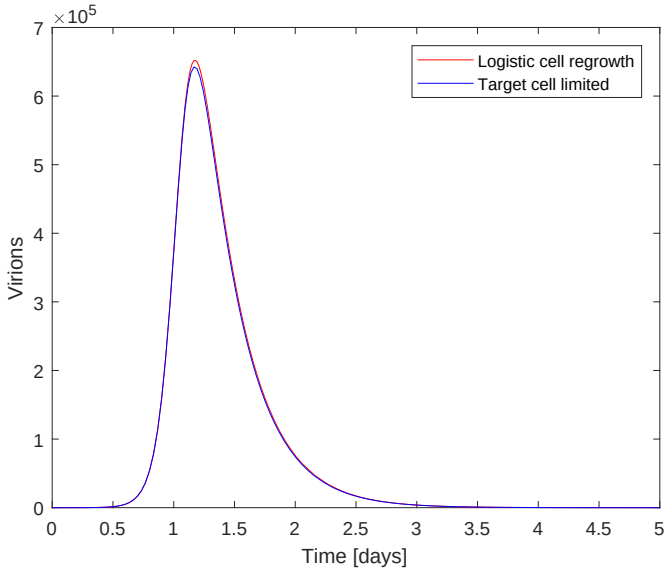

Figure 7.2

This now begs the question, how is the trough of equation 7.1 affected by parameter values? Plotting the initial trough depth versus the infectivity parameter, β, we get the following diagram

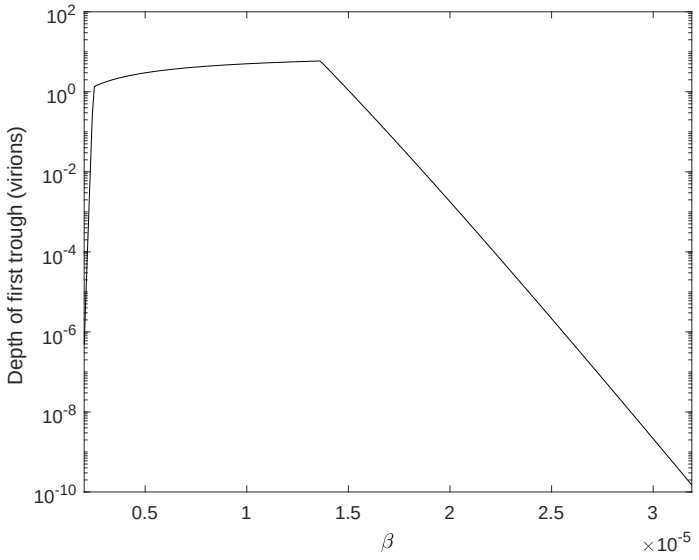

Figure 7.3

Figure 7.3 shows the initial trough depth for values of β. Here we can see that as β increases from zero, the depth of this trough gets shallower very quickly, until it plateaus and reaches a local maximum, before quickly diving down to extremely small values as β increases further. It is interesting to note that this value does not monotonically increase, but reaches some critical threshold where the trough depth quickly dives towards zero.

7.2 Stability analysis

Before undertaking analysis of the fixed points of equation 7.2 let us see how the time series behave when we vary certain parameter values.

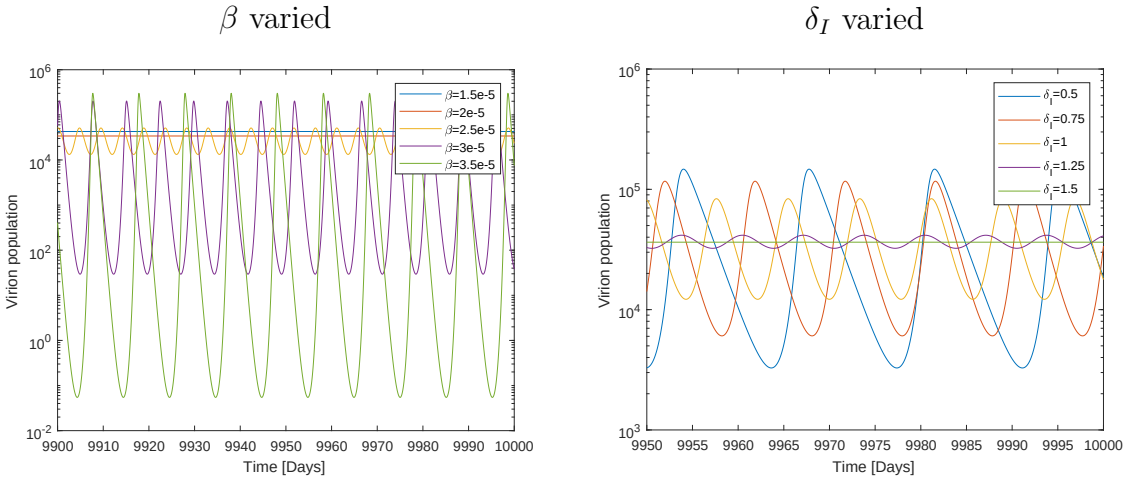

(a) (b)

Figure 7.4

As β is increased, we see the emergence of an oscillatory solution. Similarly, for δ_I decreasing, we see the emergence of oscillatory solutions. This seems to indicate the existence of limit cycles oscillating around an unstable fixed point. From this we can postulate the existence of a Hopf bifurcation with respect to each of these parameters. To test this let us perform a linear stability analysis on equation 7.2.

Once again, by inspection, we can see that there is a zero virus fixed point at $(\bar{T}, \bar{I}, \bar{V}) = (T_0, 0, 0)$. Also, similar to our derivation for the case of constant target cell regrowth, we get that there is a non-zero virus fixed point given by

$$(\bar{T}, \bar{I}, \bar{V}) = \left(\frac{c\delta_I}{p\beta}, \frac{\sigma c(p\beta T_0 - c\delta_I)}{p\beta(p\beta T_0 + \sigma c)}, \frac{p}{c}\bar{I} \right). \tag{7.3}$$

The Jacobian of equation 7.2 is given by

$$J = \begin{bmatrix} \sigma\left(1 - \frac{2T+I}{T_0}\right) - \beta V & \frac{-\sigma T}{T_0} & -\beta T \\ \beta V & -\delta_I & \beta T \\ 0 & p & -c \end{bmatrix}. \tag{7.4}$$

The characteristic polynomial of this matrix is given by

$$C(\lambda) = \lambda^3 + a_1\lambda^2 + a_2\lambda + a_3 \tag{7.5}$$

where

$$a_1 = \frac{\sigma}{T_0}I + \frac{2\sigma}{T_0}T + c + \beta V + \delta_I - \sigma, \tag{7.6a}$$

$$a_2 = \frac{c\sigma}{T_0}I + \frac{2c\sigma}{T_0}T + \frac{\beta\sigma}{T_0}TV + \frac{\delta_I\sigma}{T_0}I + \frac{2\delta\sigma}{T_0}T - p\beta T + c\beta V + c\delta_I + \beta\delta_I V - c\sigma - \delta_I\sigma, \tag{7.6b}$$

$$a_3 = \frac{\sigma}{T_0}(-p\beta IT - 2p\beta T^2 + c\beta TV + c\delta_I I + 2c\delta_I T + c\delta_I\beta T_0 V + p\beta T_0 T - c\delta_I T_0). \tag{7.6c}$$

Substituting in the value for our virus free fixed point gives

$$a_1 = c + \delta_I + \sigma, \tag{7.7a}$$

$$a_2 = c\delta_I + c\sigma + \delta_I\sigma - p\beta T_0, \tag{7.7b}$$

$$a_3 = c\delta_I\sigma - p\beta\sigma T_0. \tag{7.7c}$$

Applying the Routh-Hurwitz conditions (equation 5.9) and following the same line of logic seen in the constant target cell regrowth case, we again arrive at arrive at the condition for stability of the virus free fixed point being

$$R_0 = \frac{p\beta T_0}{c\delta_I} < 1.$$

Now we will consider the stability of the non-zero virus fixed point. Substituting in the value of our non-zero virus fixed point gives

$$a_1 = \frac{1}{\alpha(\alpha + c\sigma)}((c + \delta_I)\alpha^2 + (c^2\sigma + 2c\sigma\delta_I)\alpha + c^2\delta_I\sigma^2) \tag{7.8a}$$

$$a_2 = \frac{c\delta_I\sigma}{\alpha(\alpha + c\sigma)}((1 + \delta_I + \sigma)\alpha + c\sigma) \tag{7.8b}$$

$$a_3 = \frac{c\delta_I\sigma}{\alpha(\alpha + c\sigma)}(\alpha + c\sigma)(\alpha - c\delta_I) \tag{7.8c}$$

where $\alpha = pT_0\beta$.
Using numerical continuation software MATCONT 6p2, I was able to produce the following bifurcation diagrams for parameters β and δ_I.

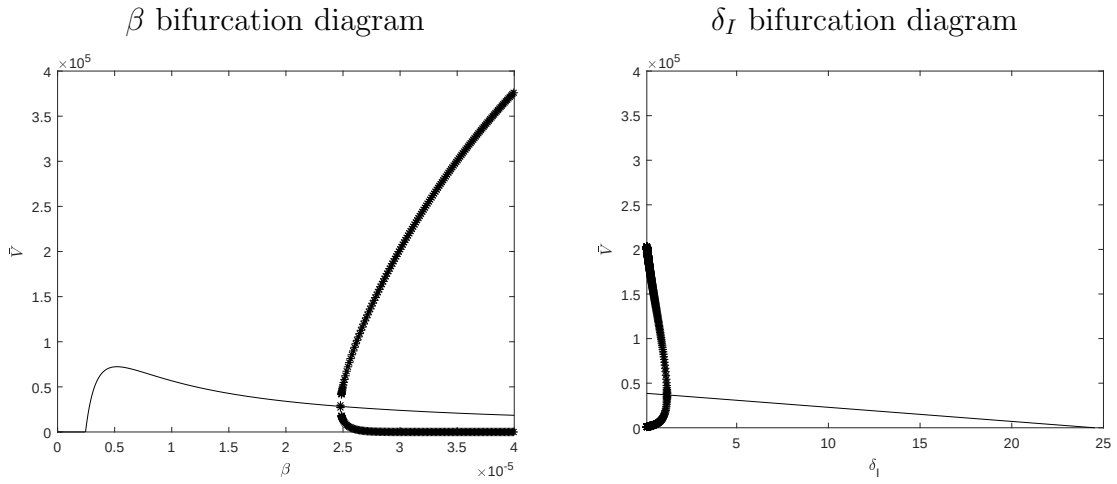

Figure 7.5: Bifurcation diagrams produced using MATCONT 6p2. For a brief description of Numerical Continuation, see Appendix A.

We can see the transcritical bifurcation point in figure 7.5a and figure 7.5b, where the zero fixed point loses stability and the non-zero fixed point gains stability. This is the point were the curve crosses the line $\bar{V} = 0$. Each curve in the respective diagrams shows the value of the equilibrium point given a particular parameter value. Looking at figure 7.5a, we can see after the transcritical bifurcation, we have an increase in the fixed point value, until some local maxima is reached, at which point it starts decreasing before a Hopf bifurcation point is reached. At this point the fixed point loses stability and limit cycle solutions emerge. The upper and lower branches show the maxima and minima of these limit cycles, respectively. As β increases, these maxima increase and the minima approach zero. Looking at figure 7.5b we can see the transcritical bifurcation point, then the value of the fixed point linearly increases as δ_I is decreased, until once again a Hopf bifurcation point is reached.

From the bifurcation curves shown in figures 7.5 and A.1, we can see that the parameters which R_0 is dependant on all undergo Hopf bifurcations. In the case of the parameters on the numerator, as they increase, stable limit cycles emerge. For the parameters in the denominator, stable limit cycles emerge as the parameter is decreased. So, as R_0 is increased, and hence the infectivity of the virus being modelled, limit cycle solutions emerge. As R_0 increases beyond this point, the peaks and troughs of the limit

cycle continue to diverge.

7.2.1 Conditions for a Hopf bifurcation

As shown in figure 7.5a, this system undergoes a Hopf bifurcation with respect to the parameter β. We know that just preceding the Hopf bifurcation point, $\beta = \bar{\beta}$, there will be 2 complex eigenvalues, $\lambda_{\pm} = f(\beta) \pm ig(\beta)$. For a Hopf bifurcation to occur, we require $f(\bar{\beta}) = 0$ where $\bar{\beta}$ is the point at which the bifurcation occurs. As previously stated, for stability of a fixed point we require $a_1 > 0$, $a_3 > 0$ and $a_1 a_2 - a_3 > 0$. As defined in in equation 7.8, we can see that $a_1 > 0$ and $a_3 > 0$ are always satisfied. Hence, we must see a qualitative change in the nature of the eigenvalues for parameter values which satisfy $a_1 a_2 - a_3 = 0$. For $\beta < \bar{\beta}$, $f(\beta) < 0$. Conversely, for $\beta > \bar{\beta}$, $f(\beta) > 0$. So we can conclude that for parameter values which satisfy $a_1 a_2 - a_3 = 0$, $f(\beta) = 0$. Our condition for a Hopf bifurcation is thus

$$a_1 a_2 - a_3 = 0 \tag{7.9}$$

Expanding out $a_1 a_2 - a_3$ and multiplying through by $\alpha^2(\alpha + c\sigma)^2)/c\delta_I\sigma$ we obtain the following polynomial equation

$$b_1\beta^4 + b_2\beta^3 + b_3\beta^2 + b_4\beta + b_5 = 0 \tag{7.10}$$

where

$$b_1 = -(pT_0)^4, \tag{7.11a}$$
$$b_2 = (pT_0)^3(c + \delta_I + 2c\delta_I + \delta_I^2 - c\sigma + \delta_I\sigma), \tag{7.11b}$$
$$b_3 = (pT_0)^2(2c^2\sigma + 3c\delta_I\sigma + 3c^2\delta_I\sigma + 2c\delta_I^2\sigma + 2c\delta_I\sigma^2), \tag{7.11c}$$
$$b_4 = pT_0(c^3\sigma^2 + 3c^2\delta_I\sigma^2 + c^3\delta_I\sigma^2 + c^2\delta_I^2\sigma^2 + c^2\delta_I\sigma^3), \tag{7.11d}$$
$$b_5 = c^3\delta_I\sigma^3. \tag{7.11e}$$

We are interested in the values of β which satisfy equation 7.10. We now use Descartes' rule of signs as described in appendix A. It is obvious by inspection that $b_2, b_3, b_4, b_5 > 0$ and $b_1 < 0$. Here, we have 1 sign difference in the sequence $(b_1, b_2, b_3, b_4, b_5)$ and hence there is one positive, real value of the parameter β that satisfies equation 7.10. This means that there is only one value of β where there is a Hopf bifurcation.
In the product defined by equation 7.9, the only instances of the parameters T_0, p and β always appear together in the product $pT_0\beta$. From this we can immediately draw the same conclusion about p and T_0, that the system only undergoes 1 Hopf bifurcation with respect to these parameters.

Substituting the baseline parameter values into the coefficients defined by equations 7.11 and then solving equation 7.10 we indeed get one real, positive root, $\beta = 2.477e{-}5$, which agrees with the value of the bifurcation point in figure 7.5a.
We can apply similar analysis to the parameters δ_I and c. Once again expanding out $a_1a_2 - a_3$ and multiplying by $\alpha^2(\alpha + c\sigma)/c\delta_I\sigma$ then grouping by powers of δ_I we get a quadratic

$$d_1\delta_I^2 + d_2\delta_I + d_3 = 0 \tag{7.12}$$

where

$$d_1 = \alpha^2 + \alpha c\sigma, \tag{7.13a}$$
$$d_2 = 3c\alpha^2 + 3\alpha c^2\sigma + \alpha^2\sigma + \alpha c\sigma + c^3\sigma^2, \tag{7.13b}$$
$$d_3 = \alpha^2c^2 + \alpha c^3\sigma - \alpha^3. \tag{7.13c}$$

$d_1 > 0$ and $d_2 > 0$ since the parameters are positive real numbers. The only way there can be a Hopf bifurcation with respect to δ_I is if $d_3 < 0$, thus giving us one sign change in the sequence (d_1, d_2, d_3). So our criteria for a Hopf bifurcation with respect to δ_I is

$$\alpha^2c^2 + \alpha c^3\sigma - \alpha^3 < 0 \tag{7.14a}$$
$$\Rightarrow \alpha c^2 + c^3\sigma - \alpha^2 < 0 \tag{7.14b}$$

In the case of the baseline parameters used in the simulation shown in figure 7.1, $d_3 = -18473000$, so we indeed do have 1 sign change in the sequence (d_1, d_2, d_3) and hence one positive value of δ_I at which a bifurcation occurs. This is not necessarily true in general however, as d_3 is not always positive for arbitrary parameter values.

Grouping by c we end up with a quartic equation

$$e_1c^4 + e_2c^3 + e_3c^2 + e_4c + e_5 = 0 \tag{7.15}$$

where

$$e_1 = \sigma^2(\alpha + \delta_I\sigma), \tag{7.16a}$$
$$e_2 = 2\alpha\sigma(\alpha + 2\delta_I\sigma), \tag{7.16b}$$
$$e_3 = \alpha^2(\alpha + 3\delta_I\sigma) + \alpha\delta_I\sigma(3\alpha + \sigma(\delta_I + \sigma)), \tag{7.16c}$$
$$e_4 = \alpha^2\sigma(-\alpha + \delta_I(\delta_I + \sigma)) + \alpha^2\delta_I(3\alpha + \sigma(\delta_I + \sigma)), \tag{7.16d}$$
$$e_5 = \alpha^3(\delta_I(\delta_I + \sigma) - \alpha)). \tag{7.16e}$$

e_1, e_2 and e_3 are all greater than zero. For our baseline parameter values, $e_4 = 9.691\text{e}8$ and $e_5 = -5.6307\text{e}10$. Thus in the sequence $(e_1, e_2, e_3, e_4, e_5)$ we have one sign change

and hence there is one positive value of c where a Hopf bifurcation occurs.

Finally, grouping by powers of σ gives us a cubic equation

$$s_1\sigma^3 + s_2\sigma^2 + s_3\sigma + s_4 = 0, \tag{7.17}$$

where

$$s_1 = c^4\delta_I + c^2\delta_I\alpha, \tag{7.18a}$$
$$s_2 = (c^4 + c^2\delta^2 + 4c^3\delta)\alpha + 2c\delta\alpha^2, \tag{7.18b}$$
$$s_3 = (2c^3 + 6c^2\delta + 2c\delta^2)\alpha^2 + (\delta - c)\alpha^3, \tag{7.18c}$$
$$s_4 = (c^2 + 3c\delta + \delta^2)\alpha^3 - \alpha^4. \tag{7.18d}$$

We can see that $s_1 > 0$ and $s_2 > 0$. Substituting in the baseline parameter values we get $s_3 > 0$ and $s_4 > 0$. Hence, we have no sign differences in the sequence (s_1, s_2, s_3, s_4) and so there will be no Hopf bifurcation with respect to σ. The fixed point diagram of the system with respect to σ.

Diagrams of the fixed points with respect to parameters that have been analysed here can bee seen in appendix A.

The system undergoes 1 Hopf bifurcation with respect to all the parameters contained in the R_0 ratio. σ cause the fixed point value of virions to increase. As it increases it asymptotically approaches some positive value of virion population.

8 Innate immune response

As with section 7, results obtained in this section were motivated by unpublished work undertaken by Ada Yan in her PhD work at the University of Melbourne.

The model given in [12] provides the groundwork for modelling innate immune response. We assume the body produces interferon at some rate proportional to the number of infected cells, and also dies at some rate proportional to the amount of interferon in the body. Interferon kills infected cells, whose interaction is governed by the law of mass action, and produces resistant target cells through interaction with target cells, again according to the law of mass action. [10] builds on this by also including a virus suppression term, in which production of virions by infected cells is suppressed according to the amount of Interferon in the body. It is important to remember that the models here are abstractions of the biology. Whilst we are referring to the specific innate immune mechanism of interferon, interferon is being used essentially as a place holder representing the entire innate immune system. For a review of models of influenza including immune response see [7].

8.1 A model of innate immune response

Here we have a model of within host viral dynamics including the innate immune response, which is a simplification of the model given in [10].

$$\frac{dT}{dt} = \sigma(T+R)\left(1 - \frac{T+R+I}{T_0}\right) - \beta TV + \rho R - \phi FT, \tag{8.1a}$$

$$\frac{dI}{dt} = \beta TV - \delta_I I - \kappa IF, \tag{8.1b}$$

$$\frac{dR}{dt} = \phi FT - \rho R, \tag{8.1c}$$

$$\frac{dV}{dt} = \frac{p}{1+sF} I - cV, \tag{8.1d}$$

$$\frac{dF}{dt} = qI - dF. \tag{8.1e}$$

We have 3 distinct mechanisms of innate immunity. Firstly, the creation of virus resistant target cells, denoted R, through a mass action interaction between target cells and innate immune cells, denoted F. The efficacy of this interaction is governed by the parameter ϕ (units $M^{-1}t$). ρ (units t^{-1}) is the rate at which resistant cells revert back to vulnerable target cells. Secondly, direct removal of infected cells from the system. This occurs via mass action interaction between infected cells and innate immune cells. This interaction governed by the parameter κ (units $M^{-1}t^{-1}$). Thirdly, decreasing the

production of virions by infected cells. The larger the amount of innate immunity cells, the greater the reduction in virion production. This mechanism is governed by parameter s (units M^{-1}). Production of innate immunity cells is stimulated by the presence of infected cells in the system, at a rate q (t^{-1}), and has a decay rate of d (t^{-1}).

T_0	V_0	σ	β	ρ	ϕ	δ_I	κ	p	s	c	q	d
7e7	10	0.8	2e-5	0.05	0.14	3	3	0.35	1	20	1e-7	2

Table 8.1

The baseline parameter values for this model are given in table 8.1 and are taken from [10]. Running a simulation with these parameters we obtain the following curves for target cells and virions.

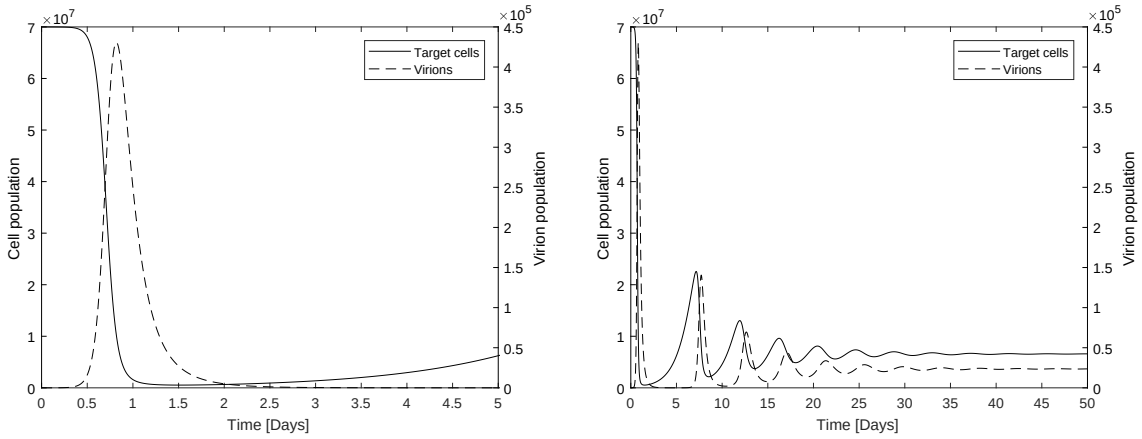

(a) (b)

Figure 8.1

We can see that a stable non-zero virus fixed point is reached very quickly, in around 40 days. Comparing this to figure 7.1b where the oscillations continue until around day 350. We can postulate that these new innate mechanisms work to dampen the oscillations in the system. We will now proceed by analysing each of the innate mechanisms separately to see what effect they have on the system. It is important to remember that the parameter values given in table 8.1 were estimated to model an acute influenza infection, so it is important to analyse their effect on the initial transient of the system as well as the long term behaviour.

In the following simulations we analyse one of κ, s or ϕ at a time and set the others to 0. The other parameters are the same as seen in table 8.1 apart from β, which has been

set to $\beta = 3\text{e-}5$. This is because the fixed point for the case $\kappa = s = \phi = 0$ (equivalent to equation 7.2) will be a limit cycle, and we wish to see how these parameters effect the limit cycle.

$$s = \phi = 0$$

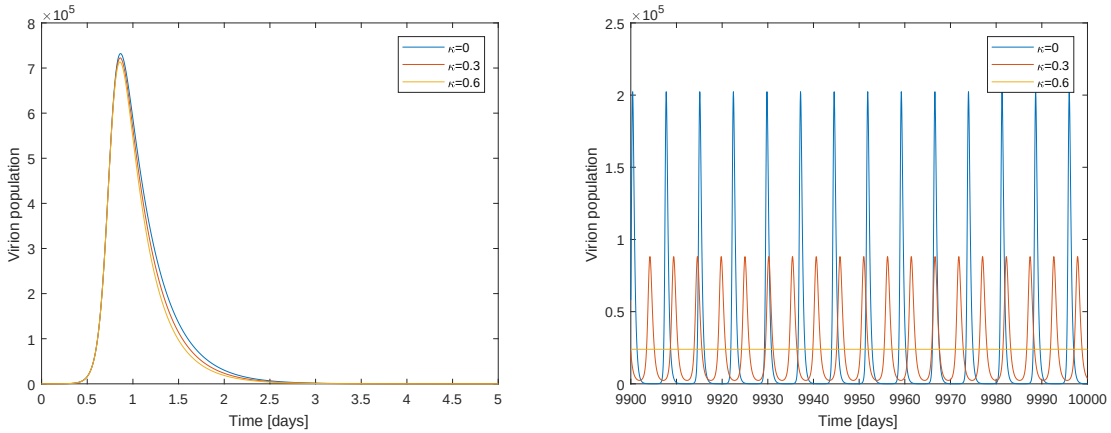

(a) (b)

Figure 8.2: Transient and long term behaviour for varied κ

$$\kappa = \phi = 0$$

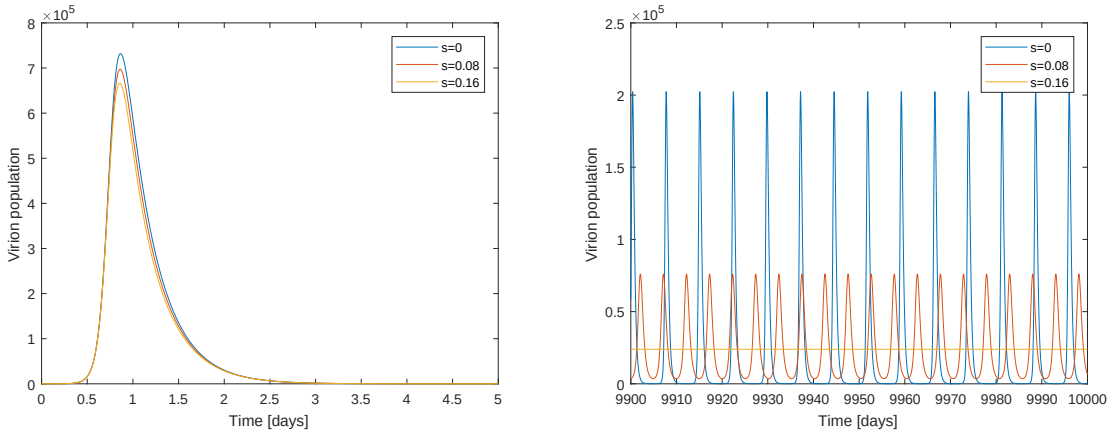

(a) (b)

Figure 8.3: Transient and long term behaviour for varied s

From figure 8.2b, 8.3b and 8.4b we can see that all of the innate immune mechanisms have the effect of dampening the oscillatory nature of the TIV model and causing the limit cycle to tend towards a stable constant fixed point. From this we expect to see a Hopf bifurcation with respect to κ, s and ϕ. Looking at the figure 8.2a and 8.3a, we can see that κ and s reduce the height of the initial peak, and cause the virus to clear

$\kappa = s = 0$

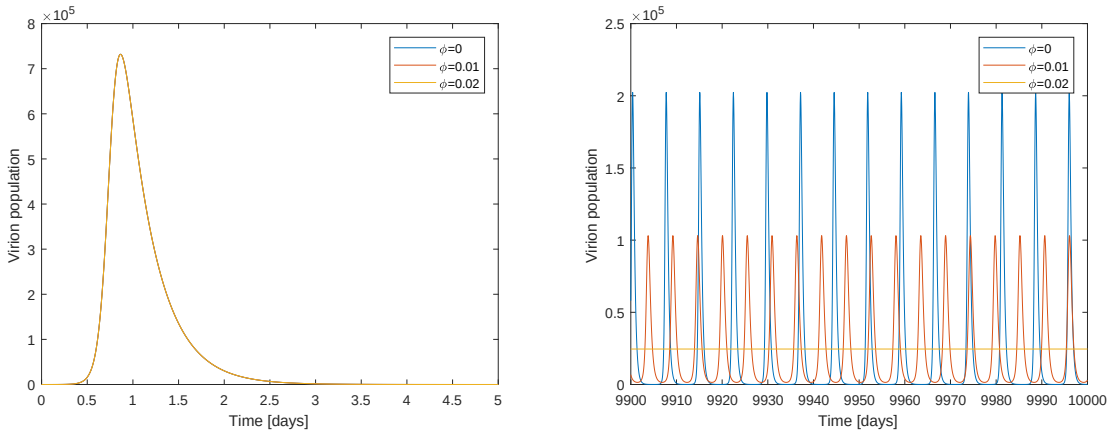

(a) (b)

Figure 8.4: Transient and long term behaviour for varied ϕ

faster. For the values of ϕ shown in 8.4a, it has no discernible impact on the initial transient.

8.1.1 Stability analysis

The only fixed point of this system that can be easily derived is the zero virus fixed point, $(T, I, R, V, F) = (T_0, 0, 0, 0, 0)$.
The Jacobian matrix of equation 8.1 is given by

$$J = \begin{bmatrix} \sigma\left(1 - \frac{2T+I+2R}{T_0}\right) - \beta V - \phi F & \frac{-\sigma(R+T)}{T_0} & \sigma\left(1 - \frac{2T+I+2R}{T_0}\right) & -\beta T & -\phi T \\ \beta V & -\delta_I - \kappa F & 0 & \beta T & -\kappa I \\ \phi F & 0 & -\rho & 0 & \phi T \\ 0 & \frac{p}{1+sF} & 0 & -c & \frac{psI}{(1+sF)^2} \\ 0 & q & 0 & 0 & -d \end{bmatrix}. \tag{8.2}$$

Now, substituting in our virus free fixed point the Jacobian simplifies to

$$J = \begin{bmatrix} -\sigma & -\sigma & -\sigma & -\beta T_0 & -\phi T_0 \\ 0 & -\delta_I & 0 & \beta T_0 & 0 \\ 0 & 0 & -\rho & 0 & \phi T_0 \\ 0 & p & 0 & -c & 0 \\ 0 & q & 0 & 0 & -d \end{bmatrix} \tag{8.3}$$

which has a characteristic polynomial given by

$$C(\lambda) = (\lambda + d)(\lambda + \sigma)(\lambda + \rho)(\lambda^2 + (c + \delta_I)\lambda + c\delta_I - p\beta T_0). \tag{8.4}$$

Our eigenvalues are given by

$$\lambda_1 = -d, \tag{8.5a}$$
$$\lambda_2 = -\sigma, \tag{8.5b}$$
$$\lambda_3 = -\rho, \tag{8.5c}$$
$$\lambda_4 = \frac{1}{2}(-c - \delta_I - \sqrt{c^2 - 2c\delta_I + \delta_I^2 - 4p\beta T_0}), \tag{8.5d}$$
$$\lambda_5 = \frac{1}{2}(-c - \delta_I + \sqrt{c^2 - 2c\delta_I + \delta_I^2 - 4p\beta T_0}). \tag{8.5e}$$

Analagous to the derivations done in section 6, in order for this fixed point to be stable we require

$$c^2 + 2c\delta_I + \delta^2 > c^2 - 2c\delta_I + \delta^2 - 4p\beta T_0$$

which again leads to

$$R_0 = \frac{p\beta T_0}{c\delta_I}.$$

So incorporation of these innate immune system mechanisms into the TIV model has no bearing on the value of R_0. Intuitively this makes sense, as the immune system variables F and R have initial conditions of 0, and hence have no impact at the initial time of infection.

Varying κ Setting $\phi = 0$ and $s = 0$ we reduce the dimension of the system to 4 as there is no effect from the resistant target cells, R. We are now able to derive a non-zero

viral fixed point to the system. This is given by

$$\bar{I} = \frac{cd\sigma(p\beta T_0 - c\delta_I)}{c^2\kappa q\sigma + dp\beta(p\beta T_0 + c\sigma)}, \tag{8.6a}$$

$$\bar{T} = T_0 - \left(\frac{\sigma c + p\beta T_0}{\sigma c}\right)\bar{I}, \tag{8.6b}$$

$$\bar{V} = \frac{p}{c}\bar{I}, \tag{8.6c}$$

$$\bar{F} = \frac{q}{d}\bar{I}. \tag{8.6d}$$

Substituting this fixed point into the Jacobian and attempting to derive some stability criteria with respect to the parameters is a somewhat futile task, as the characteristic polynomial is far too complex. So, we will proceed by doing some heuristic analysis and using numerical techniques to determine bifurcation properties.

Firstly, we notice that $\bar{I}$, $\bar{V}$ and $\bar{F}$ are all inversely proportional to κ. So as $\kappa \to \infty$, I, V and F asymptotically approach zero. However, these fixed points will never reach zero for positive κ. So whilst killing infected cells by innate immune cells reduces the value of the non-zero virus fixed point, it does not clear the virus.

Secondly, from figure 8.2b we expect a Hopf bifurcation to occur for some small value of κ. We start off with the system approaching a limit cycle until we reach some critical value of κ where the fixed point gains stability and we no longer have limit cycle solution.

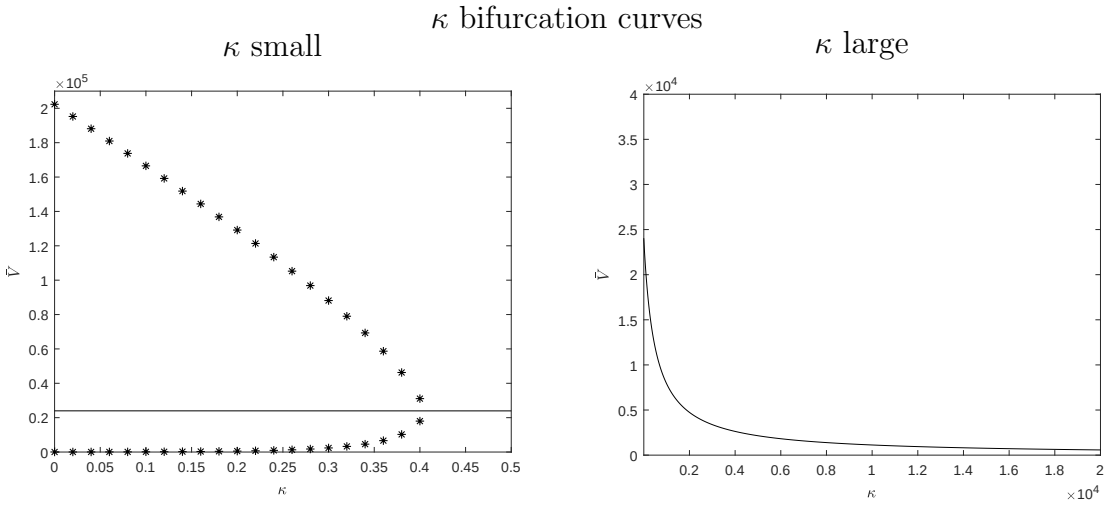

Figure 8.5: Bifurcation curves produced using MATCONT 6p2

These diagrams confirm what was stated above, we have the system tending towards a limit cycle for small values of κ before a Hopf bifurcation occurs and the fixed point gains stability. As κ gets large the fixed point tends asymptotically towards zero.

Varying s We now set $\kappa = 0$ and $\phi = 0$, again reducing the dimension of the system to 4. Figure 8.3b indicates the presence of a Hopf bifurcation. There is no simple formula for this fixed point as in the case of κ being non-zero, so we will proceed to look at the numerically produced bifurcation curves.

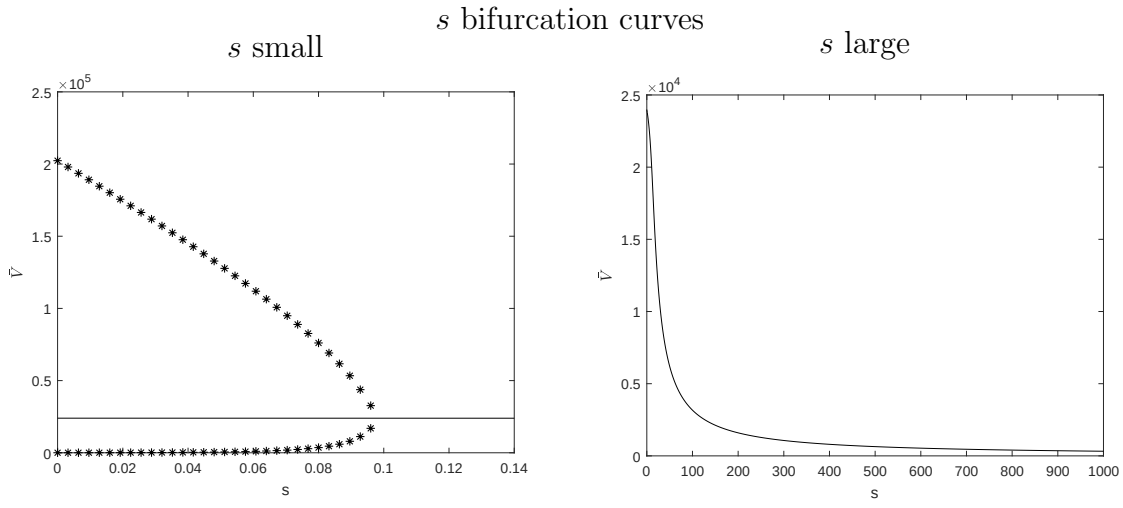

(a) (b)

Figure 8.6

Here we can see similar behaviour to that seen in the varying κ case. For very small values of s the systems tends towards a limit cycle. We then have a bifurcation point where the fixed point gains stability. As s gets large, the fixed point tends asymptotically towards zero.

Varying ϕ Thirdly, we set $\kappa = 0$ and $s = 0$. As with s, there is no simple formula for the non-zero viral fixed point.

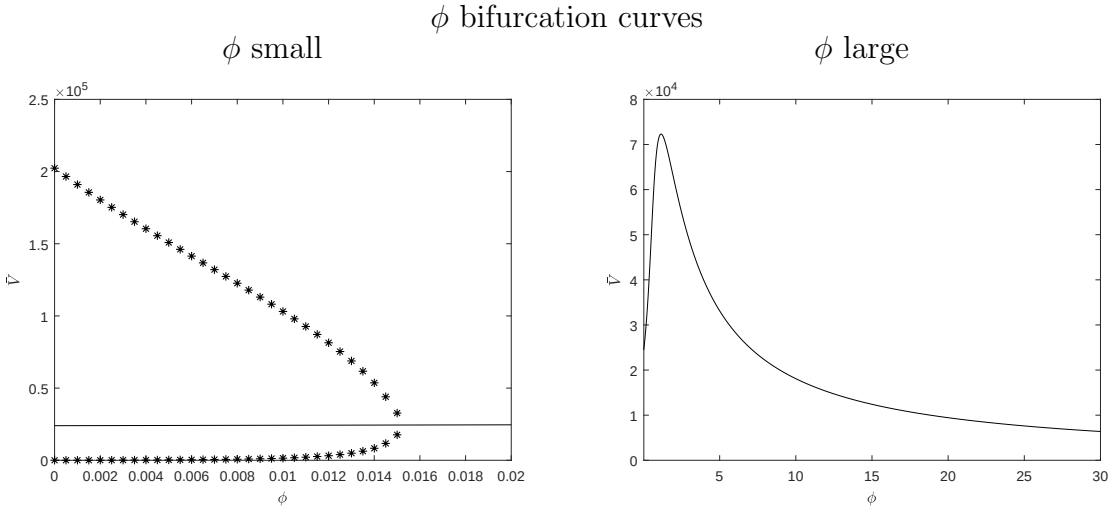

(a) (b)

Figure 8.7

Once again, we see the presence of a Hopf bifurcation bifurcation. Interestingly, though, figure 8.7b shows that increasing ϕ causes the value of the fixed point to increase, until it reaches a local maximum and then the fixed point tends asymptotically towards zero as in the previous cases.

What can we conclude from these results? Well, as postulated earlier, all three mechanisms do indeed cause the system to undergo a Hopf bifurcation, creating a stable non-zero virus fixed point. As the parameter values increase beyond the bifurcation point, direct killing of infected cells as well as slowing virion production work as expected. The non-zero virus fixed point decreases monotonically as the strength of these mechanisms increases. Creation of virus resistant cells has a different effect on the system. After the system has undergone a Hopf bifurcation the non-zero virus fixed point initially increases to a maximum before causing the fixed point to decrease to zero as the strength of this mechanism increases. Hence for small enough values of ϕ, introduction of resistant target cells to the system has the effect of increasing the infection severity.

In this analysis I have chosen not to analyse the effects of the parameters ρ, q and d. This is because we can consider their effects heuristically. Small ρ means we will have a higher ratio of resistant cells to target cells at the fixed point, and as $\rho \to 0$, at the fixed point all the healthy cells will be resistant cells. As $\rho \to \infty$, $R \to 0$ and we revert back to the TIV model with logistic target cell growth. Now, at the fixed point we also have $\bar{I} = d\bar{F}/q$. Increasing q has the same effect of reducing the number of

infected cells, and hence virions, at the fixed point, whilst increasing d has the effect of increasing the number of infected cells at the fixed point.

9 Further models

There are various compartments often included in models of within-host viral dynamics that have not been analysed here, but require mentioning as the models in section 7 and section 8 are simplifications of higher dimensional models.

9.1 Adaptive immune response

Models created and analysed by [9, 10, 11] all include adaptive immune response compartments. In [10], antibodies are included as an adaptive immune response mechanism. B cell growth is stimulated in the presence of virions. These naive (they have no effect on the virus) B cells then turn into active antibodies which kill virions via a mass action interaction. The adapted differential equations (with those not stated the same as in equation 8.1) for this adaptive mechanism are as follows,

$$\frac{dB}{dt} = m_1 V(1-B) - m_2 B, \tag{9.1a}$$

$$\frac{dA}{dt} = m_3 B - rA - \mu VA, \tag{9.1b}$$

$$\frac{dV}{dt} = \frac{pI}{1+sF} - cV - \mu VA. \tag{9.1c}$$

Naive B cells are stimulated in the presence of virions at a rate m_1 ($M^{-1}t^{-1}$) and decay at a rate m_2 (t^{-1}). The growth of these B cells is limited by the population of B cells already in the system. This works in a similar way to a logistic growth term. Then antibodies are produced at a rate m_3 (t^{-1}) proportional to B cells, and decay at a rate r (t^{-1}). There is then a mass action interaction between the antibodies and the virions in which they are both removed from the system, governed by a rate μ (t^{-1}).

The model given in [11] contains compartments for antibody response and CTL response (cytotoxic T lymphocyte, a T cell which is part of the adaptive immune response). Naive T cells produce effector T cells, which are capable of fighting off infections. In turn, the effector T cells are able to create memory T cells. These memory T cells are then able to linger in the system for an extended period of time. Hence, this model can be used to analyse the dynamics of reinfection, and the effect memory cells have on immunity to subsequent infections.

9.2 Anti-viral therapy

Models of the effects of anti-viral therapies are given in [13, 5]. The way antiviral drugs work, at a high level, are preventing the infection of new cells (reverse transcriptase

inhibitors) or by preventing infected cells from producing more virions (protease inhibitors).

As described in [5], reverse transcriptase inhibitors have the effect of decreasing β in equation 6.5, as used to model HIV infection. Similarly, protease inhibitors have the effect of reducing p in equation 6.5.

A different approach is taken in [13]. Chronic Hepatitis C infection is modelled, and the drug introduced to the system is compartmentalised. The drug then has the effect of reducing the rate of the virion/target cell interaction.

10 Discussion

In this thesis I have shown the emergence of oscillatory solutions in the TIV model with logistic target cell regrowth, how the parameters of the system affect these oscillations and the effect of incorporating an innate immune system compartment into the model. In section 6 we see that much of the dynamics of the TIV model is governed by the ratio R_0. Once logistic target cell regrowth is included in the TIV model we find some new dynamical properties. The dependence on R_0 is maintained, with the system going through a transcritical bifurcation at $R_0 = 1$. Furthermore, limit cycle solutions were shown to emerge for particular domains of all parameters, bar σ. Applying Descartes' Rule of Signs showed that there was only one Hopf bifurcation point with respect to these parameters. In this section, deriving conditions for existence of Hopf bifurcations for arbitrary parameter values was not fully explored. This is a potential area for future investigation. In section 8 we saw that the inclusion of innate immune response mechanisms has the effect of dampening oscillatory solutions in the TIV model and reducing the value of non-zero virus fixed points. κ and s dampen limit cycles until a Hopf bifurcation occurs, at which point the stable fixed point monotonically decreases as κ and s get large. Similar behaviour is noted for for ϕ, with dampening of limit cycles until a Hopf bifurcation occurs. After this point the fixed point value increases until a local maximum is reached, after which the fixed point goes to zero as ϕ gets large.

Wang [23] and Leenheer [24] have performed stability analysis on the TIV model as described in [4] and [5]. These models include either constant target cell regrowth or constant target cell and logistic target cell regrowth, and in both cases have been used to model HIV infections. In the case of constant and logistic regrowth latter both [23] and [24] have shown the existence of limit cycles solutions. This thesis has focused on models which were created to model influenza infection [9, 10, 11, 14]. As influenza is an acute infection, models of this type are calibrated so that their initial transient matches that of an influenza infection. Analysis of the long term behaviour of these models then may not lead to any great insight, as the models were not built to have their long term behaviour taken into account. However, the emergence of limit cycles is an interesting point, and perhaps suggests that these dynamics are present in influenza infections but are not fully realised, as at small virion populations stochastic behaviour dominates the dynamics and extinction occurs before the virion population can rebound. Conversely, the TIV model with logistic cell regrowth may also prove useful for modelling other viruses which feature endemic or longer term infections. Furthermore, parameter range estimations such as those given in [12] have not been taken into consideration in this thesis. Due to this, particular parameters ranges considered may be inappropriate or non-physical, even when applied to a virus other than influenza. Looking at this from

a different perspective, however, it may inferable from this thesis which parameter domains are appropriate, and choosing them such that a non-oscillatory or oscillatory solution is obtained.

The original plan in this thesis was to use the models as given in [9] and [11] as motivation for studying of the basic TIV model with logistic cell regrowth. The hypothesis was that these models would exhibit a non-zero virus steady state, from here we would be able analyse the mechanisms that have the largest effect on this fixed point. As both these models are highly complex and computationally intensive (both have 11+ states and 30+ parameters), there were numerical issues when trying to integrate these systems over long time periods, and this route was abandoned. From here the goal was to gradually increase model complexity, analysing each compartment as it is added and determining its effect on the fixed points of the system.

There is much scope for future investigation in this area. As was earlier alluded to, continuing the compartmental build up of the TIV model to a complexity seen in [9] and [11] and with consideration to the effects of each immune compartment. Analysis of the troughs displayed in the section 7 is one area of intrigue. What controls the depth of these troughs, and is there a closed form solution to determining the depth of these troughs? Another area of investigation is anti-vrial drug therapies. Lastly, in a person with a chronic infection (exemplary of a non-zero viral fixed point in a modelling context), can we introduce a drug therapy compartment to the model that will perturb the fixed point in such a way that the virus is cleared?

A Appendix

A.1 Descartes' Law of Signs

For a polynomial

$$x^n + c_1 x^{n-1} + \cdots + c_{n-2} x^2 + c_{n-1} x + c_n$$

the number of real, positive roots is equal to the number of sign differences in the sequence $(c_1, c_2, \ldots, c_{n-1}, c_n)$ or less than that number by an even number. A sign difference is if $\text{sgn}(c_i) = -\text{sgn}(c_{i+1})$ for any pair of coefficients in the sequence. The sequence must be ordered by descending power of x.

As an example, if we had a sequence of coefficients in which the signs were given by $(+, +, -, -)$, we have 1 sign difference meaning there is exactly 1 positive root to the polynomial. See [25] for further explanation.

A.2 Numerical continuation

Numerical continuation is a method of calculating fixed point values of a system of ordinary differential equations. If we run the system until a fixed point is reached for particular parameter values, using numerical continuation we can vary one of the parameters slightly and compute the value of that fixed point without having to run the simulation again.

This works by using an iterative solving method (such as Newton's method) to converge on the fixed point values when the parameter is varied slightly. Much of the issues of converging to solutions using iterative solvers is removed as we have already run the system to equilibrium, providing a close initial "guess" for the solver to use.

Numerical continuation is also capable to detecting bifurcation points in a system by analysing the eigenvalues for particular parameter values. For further explanation see [26].

A.3 Bifurcation diagrams

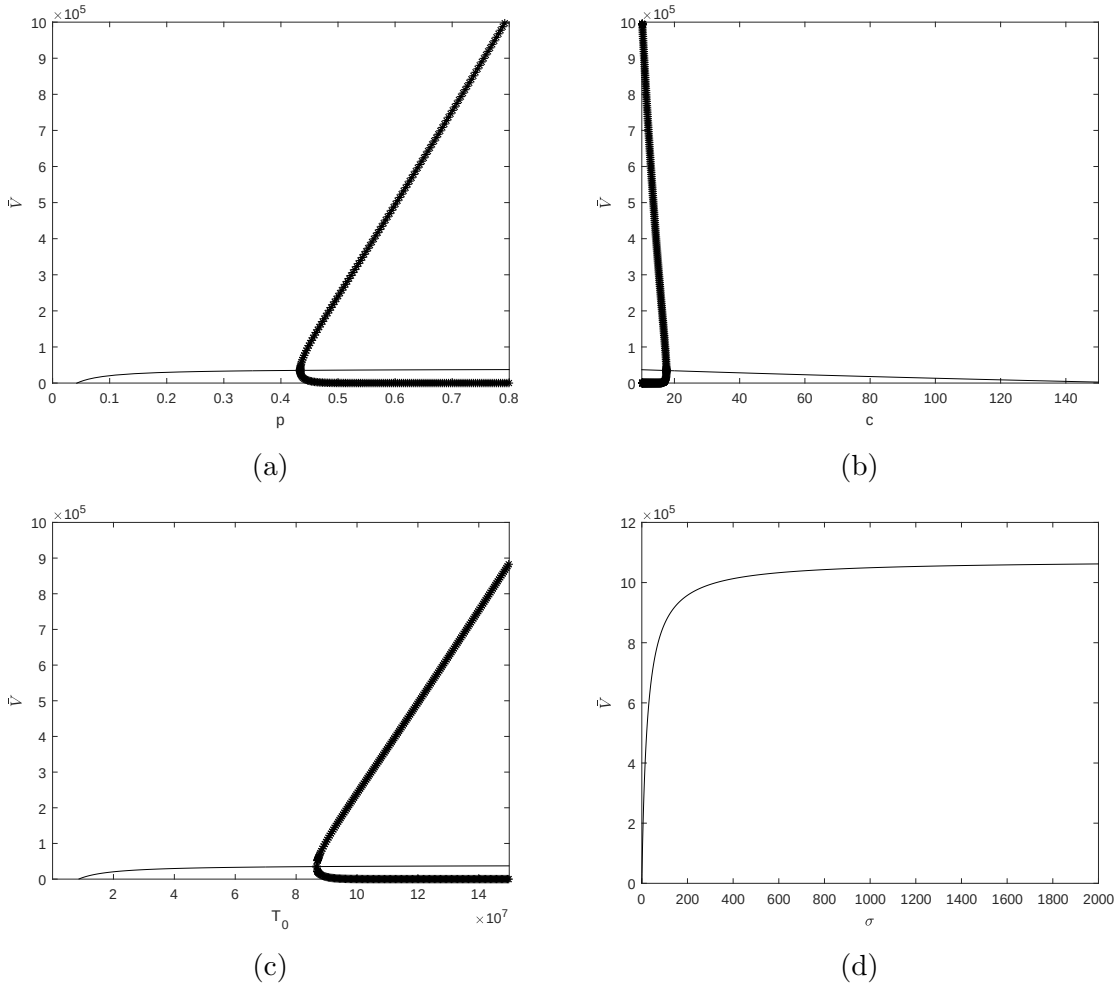

Figure A.1

References

[1] World Health Organization. *Influenza Fact Sheet 211*. URL: http://www.who.int/mediacentre/factsheets/2003/fs211/en/.

[2] World Health Organization. *HIV/AIDS Fact Sheet*. URL: http://www.who.int/en/news-room/fact-sheets/detail/hiv-aids.

[3] A. Huppert and G. Katriel. "Mathematical modelling and prediction in infectious disease epidemiology". In: *Clinicial Microbiology and Infection* 19 (2013). DOI: 10.1111/1469-0691.12308.

[4] Alan S. Perelson, Denise E. Kirschner, and Rob De Boer. "Dynamics of HIV Infection of CD4+ T cells". In: *Mathematical Biosciences* 114 (1993), pp. 81–125. DOI: 10.1016/0025-5564(93)90043-A.

[5] Martin A. Nowak and Robert M. May. *Virus Dynamics*. Great Clarendon St, Oxford: Oxford University Press, 2000.

[6] Amber M. Smith and Alan S. Perelson. "Influenza A virus infection kinetics: quantitative data and models". In: *WIREs Systems Biology and Mediciney* 8 (2011). DOI: 10.1002/wsbm.129.

[7] Hana M. Dobrovolny et al. "Assessing Mathematical Models of Influenza Infections Using Features of the Immune Response". In: *PLoS Computational Biology* 8 (2013). DOI: 10.1371/journal.pone.0057088.

[8] Andreas Handel, Ira M. Longini Jr, and Rustom Antia. "Towards a quantitative understanding of the within-host dynamics of influenza A infections". In: *Journal of the Royal Society* 7 (2009), pp. 35–47. DOI: 10.1098/rsif.2009.0067.

[9] Pengxing Cao et al. "On the Role of CD8+ T Cells in Determining Recovery Time from Influenza Virus Infection". In: *Frontiers in Immunology* 7.611 (2016). DOI: 10.3389/fimmu.2016.00611.

[10] Pengxing Cao et al. "Innate Immunity and the Inter-exposure Interval Determine the Dynamics of Secondary Influenza Virus Infection and Explain Observed Viral Hierarchies". In: *PLoS Computational Biology* 28 (2015). DOI: 10.1371/journal.pcbi.1004334.

[11] Ada W.C. Yan et al. "Modelling cross-reactivity and memory in the cellular adaptive immune response to influenza infection in the host". In: *Journal of Theoretical Biology* 413 (2017), pp. 34–49. DOI: 10.1016/j.jtbi.2016.11.008.

[12] Kasia A. Pawalek et al. "Modeling Within-Host Dynamics of Influenza Virus Infection Including Immune Response". In: *PLoS Computational Biology* 8.6 (2012). DOI: 10.1371/journal.pcbi.1002588.

[13] Laetitia Canini et al. "Impact of Different Oseltamivir Regimens on Treating Influenza A Virus Infection and Resistance Emergence: Insights from a Modelling Study". In: *PLoS Computational Biology* 10.4 (2014). DOI: 10.1371/journal.pcbi.1003568.

[14] Prasith Baccam et al. "Kinetics of Influenza A Virus Infection in Humans". In: *Journal of Virology* 80.15 (2006), pp. 7590–7599. DOI: 10.1128%2FJVI.01623-05.

[15] Lauren Sompayrac. *How Pathogenic Viruses Work*. Barb House, Barb Mews, London: Jones and Bartlett Publishers, 2002.

[16] Lauren Sompayrac. *How The Immune System Works*. The Atrium, Southern Gate, Wichester: John Wiley and Sons, 2016.

[17] Jacqueline Parkin and Bryony Cohen. "An overview of the immune system". In: *The Lancet* 357 (2001). DOI: 10.1016/S0140-6736(00)04904-7.

[18] Catherine A. A. Beauchemin and Andreas Handel. "A review of mathematical models of influenza A infections within a host or cell culture: Lessons learned and challenges..." In: *BMC Public Health* 11 (2011). DOI: 10.1186/1471-2458-11-S1-S7.

[19] Ada W. C. Yan, Pengxing Cao, and James M. McCaw. "On the extinction probability in models of within host infection: the role of latency and immunity". In: *Mathematical Biology* 73 (2016), pp. 787–813. DOI: 10.1007/s00285-015-0961-5.

[20] Steven H. Strogatz. *Nonlinear Dynamics and Chaos*. Boston, USA: Addison Wesley Publishing Company, 1994.

[21] Leah Edelstein-Keshet. *Mathematical Models in Biology*. University City, Pennsylania: Society for Industrial and Applied Mathematics, 1988.

[22] J. D. Murray. *Mathematical Biology*. 175 Fifth Avenue, New York: Springer-Verlag New York, 2002.

[23] Liancheng Wang and Michael Y. Li. "Mathematical analysis of the global dynamics of a model for HIV infection of CD4+ T cells". In: *Mathematical Biosciences* 200 (2006), pp. 44–57. DOI: 10.1016/j.mbs.2005.12.026.

[24] Patrick De Leenheer and Hal L. Smith. "Virus Dynamics: A Global Analysis". In: *Society for Industrial and Applied Mathematics* 63 (), pp. 1313–1327. DOI: 10.1137/S0036139902406905.

[25] Purple Math. *Descartes' Rule of Signs*. URL: http://www.purplemath.com/modules/drofsign.htm.

[26] Eugene L. Allgower and Kurt Georg. *Numerical Continuation Methods: An Introduction*. Berlin: Springer-Verlag, 1990.